

Synthesis of carbon nanostructures on the Fe—Mo catalysts supported on modified SiO₂

A. A. Volodin,^a P. V. Fursikov,^a Yu. A. Kasumov,^b I. I. Khodos,^b and B. P. Tarasov^{a*}

^a*Institute of Problems of Chemical Physics, Russian Academy of Sciences,
1 prosp. Akad. Semenova, 142432 Chernogolovka, Russian Federation.*

Fax: +7 (496) 515 5420. E-mail: btarasov@icp.ac.ru

^b*Institute of Problems of Technology in Microelectronics and Ultra-High-Purity Materials, Russian Academy of Sciences,
6 ul. Institutskaya, 142432 Chernogolovka, Russian Federation.*

Fax: +7 (495) 962 8047. E-mail: khodos@ipmt-hpm.ac.ru

Carbon nanostructures were synthesized by the pyrolysis of an CH₄—H₂ mixture. The synthesis was carried out on the Fe—Mo catalysts supported on the SiO₂ surface by high-frequency diode sputtering or chemical deposition from a solution of a heterometallic carbonylchalcogenide complex. Structure features of the formed carbon nanostructures affected by the size of catalytic particles, temperature of the process, and composition of the gas mixture were revealed. The presence of sulfur in the catalyst composition results in the formation of nanofibers with the bamboo-like structure.

Key words: synthesis, pyrolysis, catalyst, methane, hydrogen, carbon nanofibers, carbon nanotubes.

Carbon nanostructures (CNSs) with regular arrangement on the support find wide practical use, for instance, in molecular electronics.¹ An efficient method for syntheses of similar materials is the pyrolytic decomposition of various hydrocarbons on catalyst particles supported on a carrier (support).^{2,3} The structure and properties of carbon nanofibers (CNFs) and nanotubes (CNTs) formed in these processes depend substantially on the catalyst nature, temperature of the synthesis, and composition of the gas mixture,^{3–5} as well as on the size of particles determined by the conditions of catalyst preparation.⁶ However, the directed synthesis of carbon nanomaterials with desired structures and required physicochemical properties is of prime importance for the practical use of carbon nanomaterials. The use of supported catalysts or introduction of different additives into the catalyst composition favors the selective formation of the target product^{7–9} and an increase in its yield. For example, it is known^{10–12} that a Mo additive to the 3d-metallic catalyst enhances its catalytic activity in processes of CNF pyrolytic growth.

The purpose of the present work is the search for correlations between the parameters of the synthesis (temperature, composition of the gas mixture, size of catalytic particles) and the structures of CNFs and CNTs that formed. In addition, sulfur additives were introduced into the catalyst supported by chemical codeposition to study the sulfur effect on the growth process and structure of the prepared CNSs.

Experimental

For pyrolytic syntheses of CNFs and CNTs, the Fe—Mo catalysts supported on SiO₂ by deposition from solution or high-frequency diode sputtering were used. The method of high-frequency diode sputtering of Fe and Mo was used to obtain thin island Fe—Mo films.¹³ An advantage of this method is a possibility of film sputtering with a constant deposition rate. Plates of SiO₂ covered by a Si₃N₄ layer were used as supports. A Fe film 0.3 nm thick was sputtered on a Si₃N₄ membrane. A Mo layer with the same thickness was sputtered after a Fe layer was supported. In some cases, an Al layer was supported followed by its oxidation to Al₂O₃.

The catalyst supported on the SiO₂ plate by chemical codeposition was prepared by uniformly wetting the surface of the antidiffusional TiN_x layer covering the SiO₂ support with a saturated solution of the carbonylchalcogenide complex Cp₂MoFe₂(μ₃-S)₂(μ₃-CO)₂(CO)₆ (Cp = η-C₅H₅) followed by its drying.¹⁴

Catalytic syntheses of the carbon nanomaterials were carried out in a flow-type reactor in the temperature range from 800 to 1000 °C under atmospheric pressure using CH₄—H₂ mixtures in the mole ratios 5 : (1–3). The pyrolysis time was varied from 10 min to 1 h. The procedure of synthesis has been described in more detail in our previous study.¹⁵

Scanning and transmission electron microscopic data (SEM and TEM, respectively) were obtained with a JEOL JEM-100 CX electron microscope. The elemental composition of the supported Fe—Mo—S/TiN_x/SiO₂ catalyst was examined using a Jeol JAMP-10S Auger spectrometer. The catalyst was studied before the pyrolytic synthesis according to an earlier described¹⁶ procedure. The surface oxide layer was removed by etching the

surface with an Ar^+ ion beam with an energy of 3 keV. Ion etching was conducted until all Auger signals reached a stationary level in the region of compact arrangement of large particles. In this case, the passed depth was approximately $3.0 \times 0.5 \times 15 = 22.5$ nm. Molybdenum and iron transformed into the metallic state during two—three etching cycles. After the etching procedure, Auger spectra of the catalyst were recorded. The analysis of the Auger spectra for determining the quantitative elemental composition was performed from areas 100×100 μm in size assuming the uniform distribution in the semi-infinite matrix.

Results and Discussion

No iron islands were observed in the TEM patterns obtained after high-frequency diode sputtering of the catalyst; however, the spectra of electronic microanalysis confirmed the presence of Fe in the samples. This indicates a uniform distribution of metallic particles over the support surface. Annealing at 600—650 °C in the microscope column resulted in the formation of island Fe films with island sizes of 3—5 nm (Fig. 1, *a*). Heating the samples in an H_2 flow at the temperatures 800 and 900 °C for 10 min both with and without preliminary annealing in the electron microscope column induced the partial agglomeration of catalytic particles to form islands 5—20 nm in size (Fig. 1, *b*). At a lower annealing temperature, the size and arrangement of the islands remained virtually unchanged. Further Mo sputtering also caused some increase in the island size. The preliminary coating of the support surface with the Al_2O_3 layer (Fig. 2) prevents agglomeration of metallic particles and favors the growth of single-wall nanotubes (SNTs) because, according to published data,⁴ these tubes can grow only on small islands.

The found dependences of the characteristics of the synthesized CNTs and CNFs on the synthesis parameters can be explained in terms of the model⁵ "hydrocarbon decomposition—carbon dissolution in the catalyst particle bulk—carbon deposition."

For the mole ratio $\text{CH}_4 : \text{H}_2 = 5 : 1$ in the gas mixture at 800 °C, the CNSs grow predominantly on large particles (10—20 nm) to form many multiwall nanotubes (MNTs). No formation of nanotubes on small particles (less than 10 nm in size) was observed. In the case of small catalyst particles with the high surface to volume ratio, the rate of carbon deposition on the active surface exceeds the rate of the molar carbon flow in the particle bulk, resulting in coke formation on their active area. At 900 °C the CNS growth occurs on both large and fine particles to form a mixture of MNTs and SNTs (Fig. 3). Evidently, the temperature rise increases the rate of carbon diffusion in the catalyst bulk and, as a consequence, favors the SNT growth. The diameter of the formed MNTs ranges from 10 to 20 nm, whereas the diameter of the SNTs does not exceed 5 nm.

At 1000 °C "combined" nanostructures consisting of the SNTs covered outside by an amorphous carbon layer

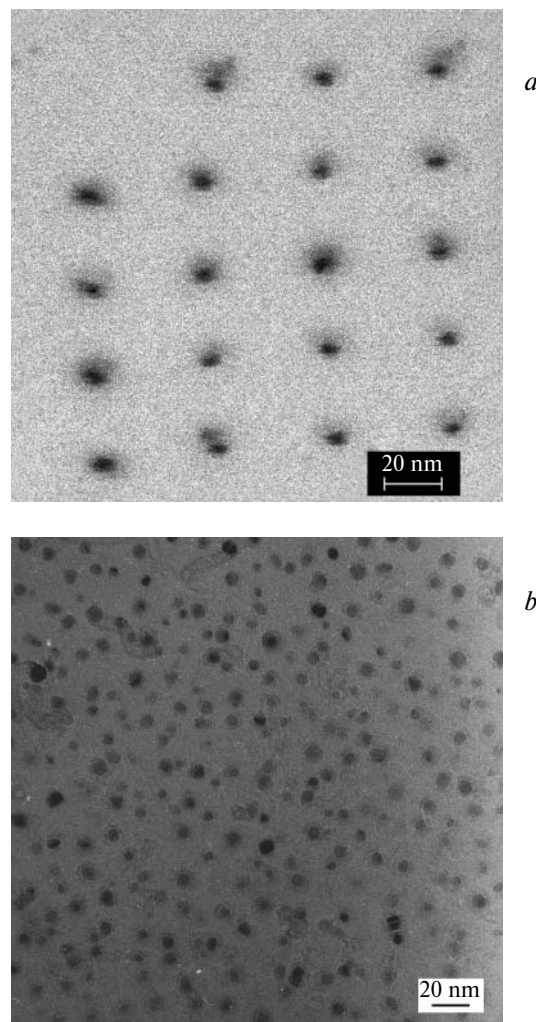


Fig. 1. Island Fe films on the $\text{SiO}_2/\text{Si}_3\text{N}_4$ support before (*a*) and after annealing at 800 °C (*b*).

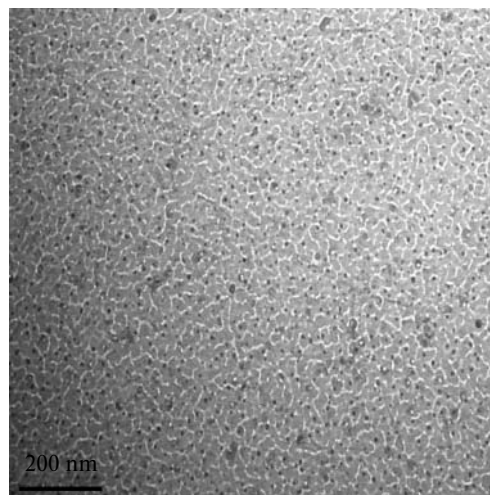


Fig. 2. Iron particles sputtered on the Al_2O_3 layer after annealing at 800 °C.

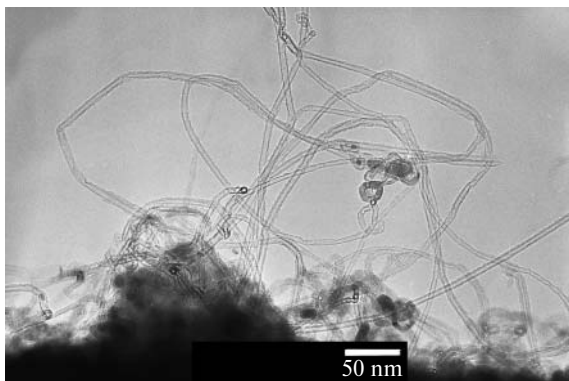


Fig. 3. Single- and multiwall nanotubes obtained by the pyrolysis of an $\text{CH}_4\text{—H}_2$ (5 : 1) mixture; 900 °C, 20 min.

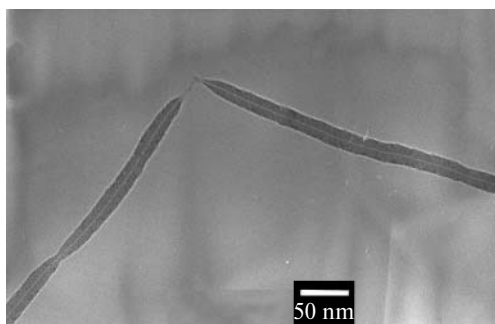


Fig. 4. Combined structures prepared by the pyrolysis of an $\text{CH}_4\text{—H}_2$ (5 : 3) mixture; 1000 °C, 20 min.

are formed (Fig. 4). Their appearance can be explained by the fact that methane is partially decomposed at this temperature on both the reactor walls and the surface of the already formed tubes to form a massive carbon "fur coat." This structure is well seen on the break of the tube found in the sample under study.

An increase in the hydrogen content in the gas mixture favors the SNT growth. For instance, at 900 °C and the ratio $\text{CH}_4 : \text{H}_2 = 5 : 3$, mainly the SNTs are formed, whose diameter is ~ 5 nm, which coincides with the diameter of catalytic particles (Fig. 5). We have earlier explained¹⁵ this effect of hydrogen. The further increase in the hydrogen content in the mixture results in the total decrease in the yield of the CNTs. This occurs, most likely, because hydrogen enters into the reaction with almost all the carbon appeared on the active catalyst surface, and equilibrium is thus strongly shifted toward gaseous products.

An increase in the pyrolysis time results in the appearance, along with the SNTs and MNTs, of spiral fibers (Fig. 6), whose growth has been observed previously.¹⁵ The model of growth of spiral nanofibers¹⁷ can be taken as a basis to explain the formation of the carbon nanospirals. According to this model, a growing fiber is curled to a spiral, because the rates of carbon deposition on

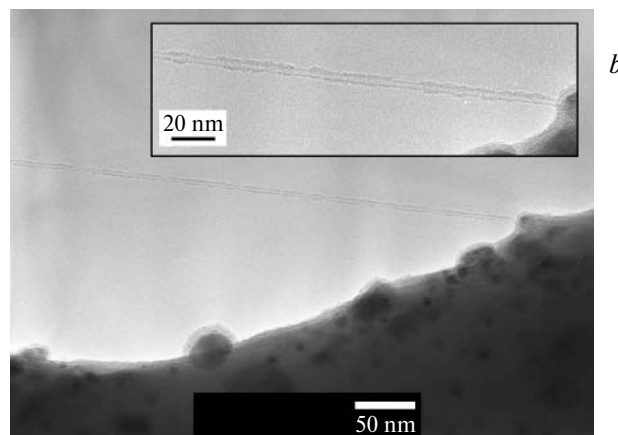
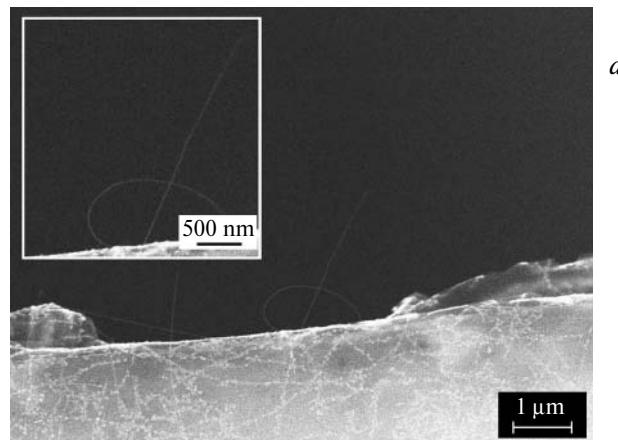


Fig. 5. SEM (a) and TEM (b) microphotographs for the SNTs obtained by the pyrolysis of an $\text{CH}_4\text{—H}_2$ (5 : 3) mixture; 900 °C, 20 min.

different faces of a catalytic particle are different due to nonisotropic diffusion of carbon in the bulk of the metallic catalyst particle. Our observations show that the diameter of the nanospirals decreases with the temperature

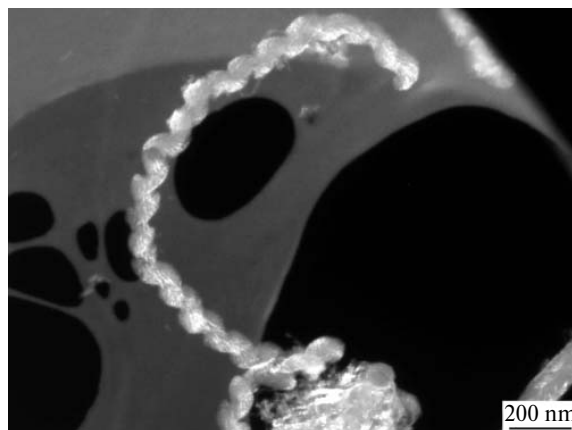


Fig. 6. Spiral fibers obtained by the pyrolysis of an $\text{CH}_4\text{—H}_2$ (5 : 3) mixture; 900 °C, 1 h.

increase. In terms of the growth model,¹⁷ this temperature dependence can be explained as follows. The diffusion coefficient of carbon in the metal in the direction specified by the vector \mathbf{n}_1 can be presented in the form $D_{\mathbf{n}_1} = A_1 \exp(-E_1/T)$, where A_1 is the pre-exponential factor, E_1 is the activation energy for diffusion in the direction \mathbf{n}_1 , and T is temperature. Therefore, for the direction \mathbf{n}_2 this coefficient is $D_{\mathbf{n}_2} = A_2 \exp(-E_2/T)$. If $E_1 > E_2$, then the $D_{\mathbf{n}_1}/D_{\mathbf{n}_2}$ ratio increases with the temperature increase resulting in a decrease in the carbon spiral diameter.

Fibers of quite different structure are formed when the sulfur-containing bimetallic Fe—Mo catalyst is used. The codeposition method from a saturated solution used in this work provides the catalyst in the form of particles ~50 nm in size. An analysis of the distribution and chemical composition of metallic particles on the support surface (Fig. 7). The signals of molybdenum and iron are present only in the Auger spectra detected in the regions with a high content of metallic particles (solid line) and correspond to the atlas of spectra of these elements. The spectral Fe : Mo ratio close to the atomic ratio of elements in the initial complex is equal to 2 : 1. Metallic particles in these regions also contain sulfur. The regions with a very low content of catalyst particles (dotted line) contain a small amount of iron, whereas Mo and S are completely absent.

The pyrolysis of an $\text{CH}_4\text{—H}_2$ (5 : 3) gas mixture on the Fe—Mo—S/TiN_x/SiO₂ catalysts results in the formation of a large amount of the CNFs covering the support surface as a "carpet." The typical microphotograph of this coating is presented in Fig. 8. However, the density of the coating is nonuniform. The analysis shows that the nanofibers grow predominantly in the regions with the high density of the catalyst. According to the TEM data, the CNFs obtained upon pyrolysis have predominantly

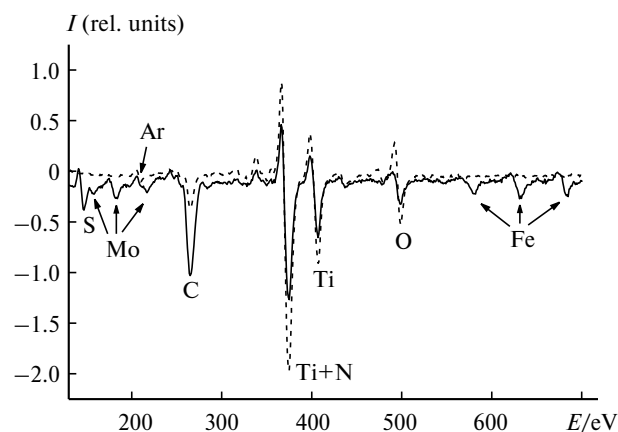


Fig. 7. Auger spectra of the initial catalyst (after its etching with an Ar^+ beam) recorded for the region with high (solid curve) and low (dotted curve) concentrations of the metallic particles.

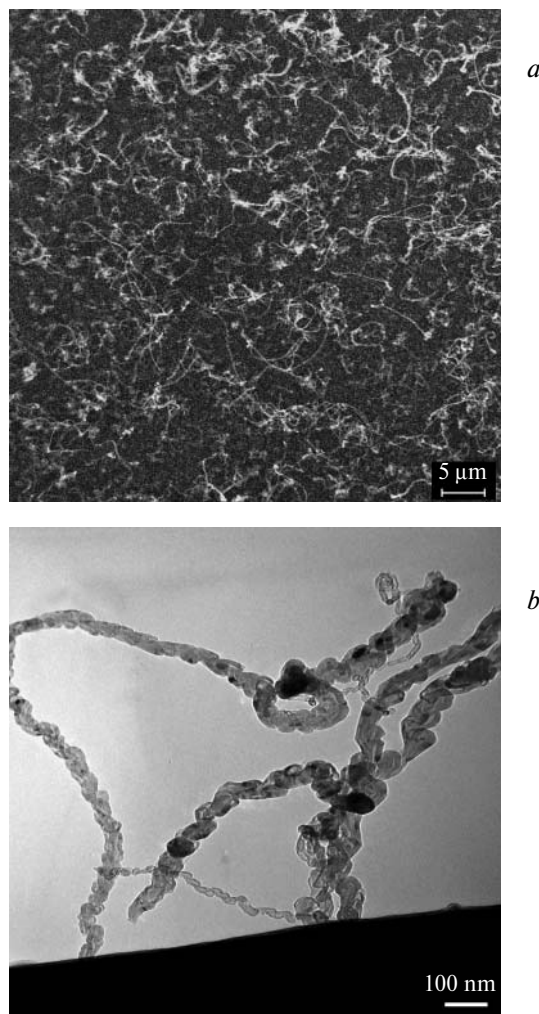


Fig. 8. SEM (a) and TEM (b) data for the pyrolysis products of an $\text{CH}_4\text{—H}_2$ (5 : 3) mixture; 900 °C, 20 min.

the so-called "bamboo-like" structure and approximately the equal length of the "bamboo fragments." This indicates that these CNFs grow periodically.

Such a periodicity of the processes that occur during the pyrolytic growth of carbon deposits on the metallic catalysts can be explained, as the authors of Ref. 5 believe, by special temperature conditions in the reaction zone and special concentrations of carbon dissolved in the metallic particles. Transitions between the corresponding regions of the metal—carbon system appear periodically during the synthesis of the CNFs. The transitions are accompanied by a change in the phase composition of the system. We propose the following explanation. Let us assume that when the system exists in the initial state at the synthesis temperature (for instance, 900 °C), a saturated solid solution of carbon is formed in a metallic particle. The carbon concentration could increase at some moment due to fluctuations. The carbon solution in the metallic particle becomes oversaturated, and excessive

carbon is rapidly precipitated to form a graphitized phase (fibers). This leads to local overheating of the particle. As a result, the limiting carbon concentration in the solid solution in this region is higher than that in the initial state, and the metal particle reaches the limiting saturation in carbon. However, the particle is cooled down gradually to the synthesis temperature and transformed again into the initial state for which the carbon content is oversaturated. An "excess" of carbon precipitates again, and the process is repeated.

The comparative analysis shows that the CNFs obtained on the bimetallic Fe—Mo catalyst containing no other additives differ sharply in structure from the nanostructures synthesized in the presence of the sulfur-containing Fe—Mo catalyst. Evidently, the presence of sulfur in the composition of the metallic particles favors the pulse growth of the CNFs with the formation of periodically repeated "bamboo-like fragments."

Thus, several conclusions can be made.

1. The island catalyst films 3–5 nm in size obtained by high-frequency diode sputtering are optimal for the synthesis of the CNTs. Annealing the support at temperatures up to 800 °C results in the partial agglomeration of catalytic particles to a size of 10–20 nm and favors the MNT growth.

2. The highest yield of the MNTs is observed at 800 °C and the ratio $\text{CH}_4 : \text{H}_2 = 5 : 1$; and an increase in the temperature and hydrogen content in the gas mixture decreases their total yield.

3. The optimal conditions of CNT formation are the temperature 900 °C and ratio $\text{CH}_4 : \text{H}_2 = 5 : 3$.

4. Particles of the catalyst Fe—Mo ~50 nm in size prepared by chemical codeposition favor the CNF growth, and the presence of sulfur in the catalyst provides the formation of fibers of the "bamboo-like" structure.

This work was financially supported by the Russian Foundation for Basic Research (Project No. 04-03-97255), the International Scientific Technical Center (Grant 2760), and the Division of Chemistry and Materials Science of the Russian Academy of Sciences (Program No. 8 "Development of Scientific Foundations of New Chemical Technologies with Preparation of Pilot Batches of Substances and Materials").

References

1. M. S. Dresselhaus, G. Dresselhaus, and Ph. Avouris, *Topics in Applied Physics*, Springer-Verlag, Berlin, 2001, 448.
2. J. Kong, H. T. Soh, A. M. Cassel, C. F. Quate, and H. Dai, *Nature*, 1998, **395**, 878.
3. P. V. Fursikov and B. P. Tarasov, *Alternativnaya Energetika i Ekologiya* [Alternative Energetics and Ecology], 2004, No. 10, 24 (in Russian).
4. P. Harris, *Carbon Nanotubes and Related Structures. New Materials for the Twenty-first Century*, University of Reading Hardback, Hardback, 1999.
5. V. V. Chesnokov and R. A. Buyanov, *Usp. Khim.*, 2000, **69**, 675 [Russ. Chem. Rev., 2000, **69** (Engl. Transl.)].
6. V. L. Kuznetsov, A. N. Usol'tseva, and Yu. V. Butenko, *Kinet. Katal.*, 2003, **44**, 791 [Kinet. Catal., 2003, **44** (Engl. Transl.)].
7. N. R. Franklin, Y. Li, R. J. Chen, A. Javey, and H. Dai, *Appl. Phys. Lett.*, 2001, **79**, 4571.
8. Y. Li, W. Kim, Y. Zhang, M. Rolandi, D. Wang, and H. Dai, *J. Phys. Chem. B*, 2001, **105**, 11424.
9. C. L. Cheung, A. Kurtz, H. Park, and C. M. Lieber, *J. Phys. Chem. B*, 2002, **106**, 2429.
10. A. R. Harutyunyan, B. K. Pradhan, and U. J. Kim, *Nanotechnology*, 2002, **2**, 525.
11. Y. Li, J. Liu, Q. Wang, and Z. L. Wang, *Chem. Mater.*, 2001, **13**, 1008.
12. B. C. Liu, S. C. Lyu, and S. I. Jung, *Chem. Phys. Lett.*, 2004, **383**, 104.
13. Yu. A. Kasumov, I. I. Khodos, V. T. Volkov, V. N. Matveev, A. Yu. Kasumov, B. P. Tarasov, A. A. Volodin, P. V. Fursikov, and O. N. Efimov, *Tez. dokl. XX Ros. konf. po elektronnoi mikroskopii* (Chernogolovka, June 1–4, 2004) [Abstrs XX Russian Conference on Electronic Microscopy], Noginsk, 2004, 6 (in Russian).
14. A. A. Pasynskii, Zh. V. Dobrokhotova, and N. I. Semenova, *Izv. Akad. Nauk, Ser. Khim.*, 2003, 103 [Russ. Chem. Bull., Int. Ed., 2005, **54**, 109].
15. A. A. Volodin, P. V. Fursikov, Yu. A. Kasumov, I. I. Khodos, and B. P. Tarasov, *Izv. Akad. Nauk, Ser. Khim.*, 2005, 2210 [Russ. Chem. Bull., Int. Ed., 2003, **52**, 2281].
16. V. G. Beshenkov, A. G. Znamenskii, and V. A. Marchenko, *Izv. Akad. Nauk, Ser. Fiz.* [Physical Bulletin of the Russian Academy of Sciences], 1998, 517 (in Russian).
17. Y. Wen and Z. Shen, *Carbon*, 2001, **39**, 2369.

Received June 28, 2006